Identification and Isolation of Small CD44-Negative Mesenchymal Stem/Progenitor Cells From Human Bone Marrow Using Elutriation and Polychromatic Flow Cytometry

Sean R.R. Hall, Yajuan Jiang, Elizabeth Leary, Greg Yavanian, Sarah Eminli, David W. O'Neill and Wayne A. Marasco

Stem Cells Trans Med 2013, 2:567-578.
doi: 10.5966/sctm.2012-0155 originally published online July 11, 2013

STEM CELLS TRANSLATIONAL MEDICINE

TISSUE-SPECIFIC PROGENITOR AND STEM CELLS

Identification and Isolation of Small CD44-Negative Mesenchymal Stem/Progenitor Cells From Human Bone Marrow Using Elutriation and Polychromatic Flow Cytometry

SEAN R.R. HALL,[a] YAJUAN JIANG,[a] ELIZABETH LEARY,[a] GREG YAVANIAN,[a] SARAH EMINLI,[a] DAVID W. O'NEILL,[a] WAYNE A. MARASCO[b]

Key Words. CD44 • Elutriation • FACS • Mesenchymal progenitor cells • Bone marrow

[a]NeoStem Inc., Cambridge, Massachusetts, USA; [b]Department of Cancer Immunology and AIDS, Dana-Farber Cancer Institute, Harvard Medical School, Boston, Massachusetts, USA

Correspondence: David W. O'Neill, M.D., NeoStem, Inc., 420 Lexington Avenue, Suite 450, New York, New York 10170, USA. Telephone: 212-584-4180; Fax: 646-514-7787; E-Mail: doneill@progenitorcell.net; or Wayne A. Marasco, M.D., Ph.D., Department of Cancer Immunology and AIDS, Dana-Farber Cancer Institute, Harvard Medical School, 450 Brookline Avenue, Boston, Massachusetts 02215, USA. Telephone: 617-632-2153; Fax: 617-632-3889; E-Mail: wayne_marasco@dfci.harvard.edu

Received November 15, 2012; accepted for publication March 28, 2013; first published online in SCTM *Express* July 11, 2013.

1066-5099/2013/$20.00/0

http://dx.doi.org/10.5966/sctm.2012-0155

ABSTRACT

The method of isolation of bone marrow (BM) mesenchymal stem/stromal cells (MSCs) is a limiting factor in their study and therapeutic use. MSCs are typically expanded from BM cells selected on the basis of their adherence to plastic, which results in a heterogeneous population of cells. Prospective identification of the antigenic profile of the MSC population(s) in BM that gives rise to cells with MSC activity in vitro would allow the preparation of very pure populations of MSCs for research or clinical use. To address this issue, we used polychromatic flow cytometry and counterflow centrifugal elutriation to identify a phenotypically distinct population of mesenchymal stem/progenitor cells (MSPCs) within human BM. The MSPC activity resided within a population of rare, small $CD45^-CD73^+CD90^+CD105^+$ cells that lack CD44, an antigen that is highly expressed on culture-expanded MSCs. In culture, these MSPCs adhere to plastic, rapidly proliferate, and acquire CD44 expression. They form colony forming units-fibroblast and are able to differentiate into osteoblasts, chondrocytes, and adipocytes under defined in vitro conditions. Their acquired expression of CD44 can be partially downregulated by treatment with recombinant human granulocyte-colony stimulating factor, a response not found in BM-MSCs derived from conventional plastic adherence methods. These observations indicate that MSPCs within human BM are rare, small $CD45^-CD73^+CD90^+CD105^+$ cells that lack expression of CD44. These MSPCs give rise to MSCs that have phenotypic and functional properties that are distinct from those of BM-MSCs purified by plastic adherence. STEM CELLS TRANSLATIONAL MEDICINE *2013;2:567–578*

INTRODUCTION

Mesenchymal stem/stromal cells (MSCs) are rare, nonhematopoietic adult stem cells originally found to reside in bone marrow (BM) [1, 2]. These plastic-adherent cells were originally characterized by their ability to (a) give rise to the colony forming unit-fibroblast (CFU-F), (b) support hematopoiesis, and (c) possess osteogenic potential [3, 4]. MSCs have been isolated successfully from a number of non-BM tissue sources, including dental pulp [5], lung [6, 7], adipose tissue [8], placenta [9], and umbilical cord [10]; however, BM is still the most extensively studied source to date [11]. Because of the ease of isolating them from BM, expansion capability in vitro, and differentiation potential and immunomodulatory properties, MSCs represent a promising cell-based therapy option for enhancing endogenous tissue repair [12–14] and suppressing autoimmunity [15–17].

BM-MSCs are rare cells, with an estimated frequency of 1 in every 10,000–100,000 nucleated BM cells [18]. Although MSCs have been suggested to occupy a perivascular niche in the BM [19], there is a paucity of data pertaining to the physical characteristics and antigenic profile of the candidate progenitor population in vivo that gives rise to cultured MSCs. Moreover, cultured MSCs represent a heterogeneous population of cells [20, 21], as they are expanded from plastic-adherent cells obtained from unfractionated BM, which contains a number of other cell types that have the ability to adhere to a plastic surface, including endothelial cells, fibroblasts, and monocytes.

There is great interest in the in vivo identification of MSCs. Despite an emerging consensus regarding the topography of MSCs within the BM [19], there is a lack of agreement regarding their antigenic profile [22]. This is related to the fact that the antigenic profile of MSCs has been elucidated postculture in an artificial environment. However, using a limited set of markers, a number of studies have attempted to identify the immunophenotype of prospectively isolated cells that subsequently behave as MSCs in culture [22, 23]. One

of the markers, CD271, has received considerable attention, as it has been used to isolate cells from BM with MSC-like properties [24–26]. However, even within this population there is a lack of accord on the antigenic profile [22]. Indeed, there is a growing need within the MSC field, similar to the evolving hematopoietic stem cell (HSC) [27] and endothelial progenitor cell fields [28], to develop expanded antibody panels (involving four or more surface markers) for the prospective identification and purification of unique BM mesenchymal stem and progenitor cell (MSPC) populations. This approach would apply to therapeutic applications as well as for basic research, since the identity of the isolated MSPC population may be linked to its efficacy for specific clinical applications, such as regenerative or immunomodulatory therapies [22].

In addition to immunomagnetic- or fluorescence-activated cell sorting (FACS), counterflow centrifugal elutriation (CCE) represents an alternative approach for the separation and enrichment of cells on the basis of their size and cell mass [29]. The concept of using elutriation for cell separation was first introduced by Lindahl [30, 31]. For clinical applications, CCE has been used to enrich monocytes from a large volume of peripheral blood mononuclear cells [32]. Recently, there has been interest in CCE as a method to separate lymphocyte subpopulations from monocytes and granulocytes [33], as well as to enrich tumor cell [34] and progenitor cell populations [35]. Primitive progenitors within mouse BM have been isolated using CCE from the earliest elutriated fractions on the basis of size and shown to contribute to lymphohematopoietic reconstitution [36], as well as multilineage engraftment to epithelial tissues in recipient mice [37]. However, to our knowledge, whether CCE can be used to isolate and identify early primitive cells within human BM with mesenchymal potential is not known.

In the present study, a five-antibody marker panel, which included CD45, CD73, CD90, CD105, and CD44, representing several of the most commonly used markers for immunophenotypic analysis of culture-expanded MSCs, was used to prospectively isolate BM MSPCs that display MSC activity in culture. Surprisingly, MSC activity was found to reside in a population of small, $CD45^-CD73^+CD90^+CD105^+$ cells that lacked expression of CD44s, the standard isoform of the CD44 cell adhesion molecule that is commonly used to identify MSCs. These rare $CD45^-CD73^+CD90^+CD105^+CD44^-$ MSPCs, which were between 5 and 12 μm in diameter, expanded rapidly in culture and demonstrated trilineage mesenchymal differentiation potential into osteoblasts, chondrocytes, and adipocytes in vitro. By CCE, these rare, small $CD44^-$ cells cofractionated with lymphocytes and were easily separated from plastic-adherent monocytes. Following expansion, the cells displayed phenotypic markers commonly associated with MSCs, including acquisition of CD44. These observations demonstrate that human BM contains a previously undescribed population of small MSPCs that lack expression of CD44. Isolation of these MSPCs to a high level of purity combined with ease of ex vivo expansion will enable their further characterization and comparison with conventional plastic-adherent MSCs for clinical applications of tissue regeneration and immune modulation.

Materials and Methods

Sample Processing

Fresh, unprocessed BM was obtained from healthy donors (Lonza, Walkersville, MD, http://www.lonza.com). Samples were processed under aseptic conditions. After red blood cell lysis (Pharm Lyse 1× lysis buffer; BD Pharmingen, San Diego, CA, http://www.bdbiosciences.com), cells were washed with 0.5% human serum albumin (HSA) in Dulbecco's phosphate-buffered saline (DPBS) and centrifuged at 680*g* for 15 minutes at 4°C. Next, cells were counted for viability and resuspended in 0.5% HSA/DPBS and processed for cell isolation. Fresh, mobilized leukapheresis products were purchased from AllCells (Emeryville, CA, http://www.allcells.com) or collected from healthy volunteers at NeoStem Laboratory (Cambridge, MA, http://www.neostem.com) under an institutional review board-approved protocol. Three days prior to apheresis, healthy donors received daily subcutaneous injections of granulocyte-colony stimulating factor (G-CSF) (480 μg/day; Neupogen; Amgen, Thousand Oaks, CA, http://www.amgen.com). A certified staff technician conducted the collection of the apheresis product over the course of 2–3 hours. After the collection of the mobilized apheresis product, cells were diluted to a final concentration of 2.5×10^8 cells per milliliter in 300 ml of 0.5% HSA/phosphate-buffered saline (PBS) prior to elutriation as described below.

Fluorescence-Activated Cell Sorting

After cell viability of the lysed BM was determined, CD34- and CD133-expressing cells were depleted using MACS CD34 and CD133 microbead kits (Miltenyi Biotec, Bergisch Gladbach, Germany, http://www.miltenyibiotec.com) performed with the MACS LS column and QuadroMACS separator (Miltenyi Biotech) according to the manufacturer's instructions. Both the enriched and the depleted fractions were examined for cell viability, cell number, and cell size distribution using a Cellometer analyzer (Nexcelom Biosciences, Lawrence, MA, http://www.nexcelom.com). CD34/CD133-depleted fractions were resuspended in FACS staining buffer (R&D Systems Inc., Minneapolis, MN, http://www.rndsystems.com) and incubated with the following antibodies: CD45-Pacific blue (Beckman Coulter, Fullerton, CA, http://www.beckmancoulter.com), CD73-allophycocyanin (APC; BD Biosciences, San Diego, CA, http://www.bdbiosciences.com), CD90-fluorescein isothiocyanate (BD Biosciences), CD105-phycoerythrin (PE; BD Biosciences), and CD44-APC-H7 (BD Biosciences) on ice for 30 minutes. Following staining, cells were washed with DPBS, centrifuged at 680*g* for 10 minutes, resuspended in buffer, and passed through a 40-μm filter (BD Biosciences). The viability dye 7-aminoactinomycin D (7-AAD; Beckman Coulter) was added prior to sorting.

Cell sorting was carried out with a high-speed Moflo XDP cell sorter (Beckman Coulter). The Moflo XDP was equipped with four lasers (488, 642, 405, and 355 nm). The forward scatter threshold was carefully set low to ensure inclusion of small cells. Cells were analyzed and sorted using a sequential gating strategy. An initial gate was set on CD45 versus 7-AAD, where $CD45^-$ live ($7\text{-}AAD^-$) cells were then displayed on a CD73 versus CD90 plot, and then a second gate was drawn to include the cluster of $CD73^+CD90^+$ cells. Following this, $CD45^-CD73^+CD90^+$ viable cells were further applied on a third plot of CD105 versus CD44 with quadrant gates delineated for $CD105^+$ or $CD44^+$ cells. Populations of the following four (if any) $CD45^-/CD73^+/CD90^+/CD105^+/CD44^-$, $CD45^-/CD73^+/CD90^+/CD105^+/CD44^+$, $CD45^-/CD73^+/CD90^+/CD105^-/CD44^-$, and $CD45^-/CD73^+/CD90^+/CD105^-/CD44^+$ were sorted directly to tubes containing ice-cold (4°C) chemically defined, serum-free culture medium (MSCGM-CD; Lonza). Cells from the population of $CD45^-/CD73^+/CD90^+/$

$CD105^+/CD44^-$ were also back-gated and displayed again on a side scatter/forward scatter (SSC/FSC) color density plot to reveal their location, and standardized flow cytometric beads were used to confirm their size (supplemental online data).

The sorted cells were centrifuged at 680*g* for 15 minutes at 4°C, resuspended in MSCGM-CD and seeded into either six-well or 10-cm dishes. Cultures were maintained in a humidified incubator with 5% CO_2 and low oxygen (5% O_2) at 37°C. The cells were left untouched for 5 days. On day 6 nonadherent cells were aspirated off, and then fresh MSCGM-CD medium was added. Following this, adherent cultures were maintained by changing the medium twice weekly. The cultures were continuously fed for 10–14 days until they reached 70%–80% confluence. Cells were expanded following subculturing and used for differentiation assays and flow cytometric analysis as described below. Unstained cells and isotype negative control samples were used to set photomultiplier voltage for baseline fluorescence and to set quadrant statistics for analyzing positive fluorescence above baseline. Compensation was manually adjusted using known positive single color-stained samples together with an unstained control. Data acquisition and analysis were performed using Summit software (Beckman Coulter). A minimum of 500,000 events were recorded as a list mode file for further analysis.

Enrichment of $CD44^-$ Bone Marrow Stem/Progenitor Cells by Elutriation

The Elutra cell separation system (CaridianBCT, Lakewood, CO, http://www.caridianbct.com) uses CCE and was programmed to enrich the different cell types based primarily on size and secondarily on density to separate populations of cells into more specific cell fractions. Briefly, approximately $2–3 \times 10^8$ nucleated cells from lysed BM were resuspended in 100 ml of 0.5% HSA/DPBS and loaded onto the Elutra system. Lysed BM cells or apheresis products (see above for details) were fractionated under a constant centrifugation rate of 2,400 rpm, and five successive elutriated fractions of 450–900 ml were collected in 0.5% HSA/DPBS using progressive increases in pump speed. Each collected fraction was centrifuged at 680*g* for 20 minutes at 4°C to pellet the cells. Elutriated cells were used for CD34/CD133 depletion and FACS as described above.

Density Gradient/Plastic Adherence Conventional Method to Isolate Bone Marrow MSPCs

Mononuclear cells (MNCs) from donor-matched BM were isolated by Ficoll density gradient fractionation (Ficoll-Paque Premium, 1.077; GE Healthcare, Little Chalfont, U.K., http://www.gehealthcare.com). MNCs were carefully removed, washed, and resuspended MSCGM-CD (Lonza) or culture medium composed of α-minimal essential medium (αMEM)/GlutaMAX (Gibco, Grand Island, NY, http://www.invitrogen.com) with 10% fetal bovine serum (FBS; Invitrogen, Carlsbad, CA, http://www.invitrogen.com). Following enumeration of MNCs, cells were plated onto plastic dishes at a ratio of 1.0×10^6 cells per cm^2 growth area in MSCGM-CD or αMEM/GlutaMAX with 10% FBS. Cultures were maintained in a humidified incubator with 5% CO_2 and low oxygen (5% O_2)at 37°C. After 72 hours, nonadherent cells were aspirated off, the adherent cells were washed with 5 ml of prewarmed PBS, and then fresh MSCGM-CD medium or αMEM/GlutaMAX with 10% FBS culture medium was added. Following this, adherent cultures were maintained by changing the medium twice weekly. The cultures were continuously fed for 10–14 days until they reached 70%–80% confluence. Cells were expanded following subculturing and used for differentiation assays and flow cytometric analysis as described below.

CFU-F

To examine the CFU-F potential of the elutriated fractions prior to FACS, 1.0 cell per cm^2 was plated in a six-well dish in MSCGM-CD. Cells were grown for 14 days; thereafter, the medium was removed and cells were washed with DPBS, fixed with methanol (BDH) for 5 minutes at room temperature. Next, the methanol was removed, and cells were air dried for 5 minutes at room temperature. To stain cultures, 2 ml of Giemsa (EMD Chemicals, Billerica, MA, http://emdmillipore.com) staining solution was added to each well and incubated for 10 minutes at room temperature. Afterward, the staining solution was removed and cells were washed with distilled water to remove unbound stain and further washed until wells were clear.

Adipogenic, Chondrogenic, and Osteogenic Differentiation

Culture-expanded (passage 3) cells were grown in defined in vitro culture conditions to examine their multipotentiality toward the mesenchymal lineage, as previously described. Briefly, following 3 weeks of standard culture conditions for adipogenesis, cells were fixed and stained with Oil Red O (Sigma-Aldrich, St. Louis, MO, http://www.sigmaaldrich.com). Following the extraction of Oil Red O using 70% isopropanol, the supernatant was measured spectrophotometrically at 510 nm to quantify adipogenesis. To induce chondrogenesis, cell pellets were formed and grown in chondrogenic induction medium (Lonza) supplemented with 10 ng/ml of transforming growth factor-β3 (Lonza). After 21 days, the cell pellets were fixed in 10% formalin and stained with safranin-O (Sigma-Aldrich). To induce osteogenesis, cells were grown in osteogenic induction medium. After 21 days, cells were fixed with 10% formalin and stained with 40 mM alizarin red S (Sigma-Aldrich) (pH 4.2).

Single-Color Flow Cytometric Analysis of Culture-Expanded Cells

Immunophenotypic analysis of culture-expanded (passage 3) FACS-sorted or elutriation/FACS-sorted cells and donor-matched MSCs was performed using a Gallios flow cytometer (Beckman Coulter). For analysis, 30,000 events were collected and analyzed using Kaluza software (Beckman Coulter). A list of the antibodies used is given in supplemental online Table 1.

G-CSF Treatment

To examine the effects of G-CSF treatment on the cell surface phenotype of elutriated/FACS-sorted cells versus BM-MSCs isolated using conventional methods, cells were treated with 10 ng/ml recombinant human G-CSF (R&D Systems) for 4 consecutive days in serum-free αMEM/GlutaMAX medium. Following treatment, cells were harvested using HyQTase, counted and resuspended in 100 μl of staining buffer with CD105-PE and CD44-APC-H7 for 15 minutes on ice. Flow cytometric analysis was performed using a Gallios flow cytometer (Beckman Coulter), and 50,000 events were collected and analyzed using Kaluzza software (Beckman Coulter).

Statistical Analysis

All results were expressed as mean ± SEM. One-way analysis of variance and post hoc Student-Neuman-Keuls was used on data

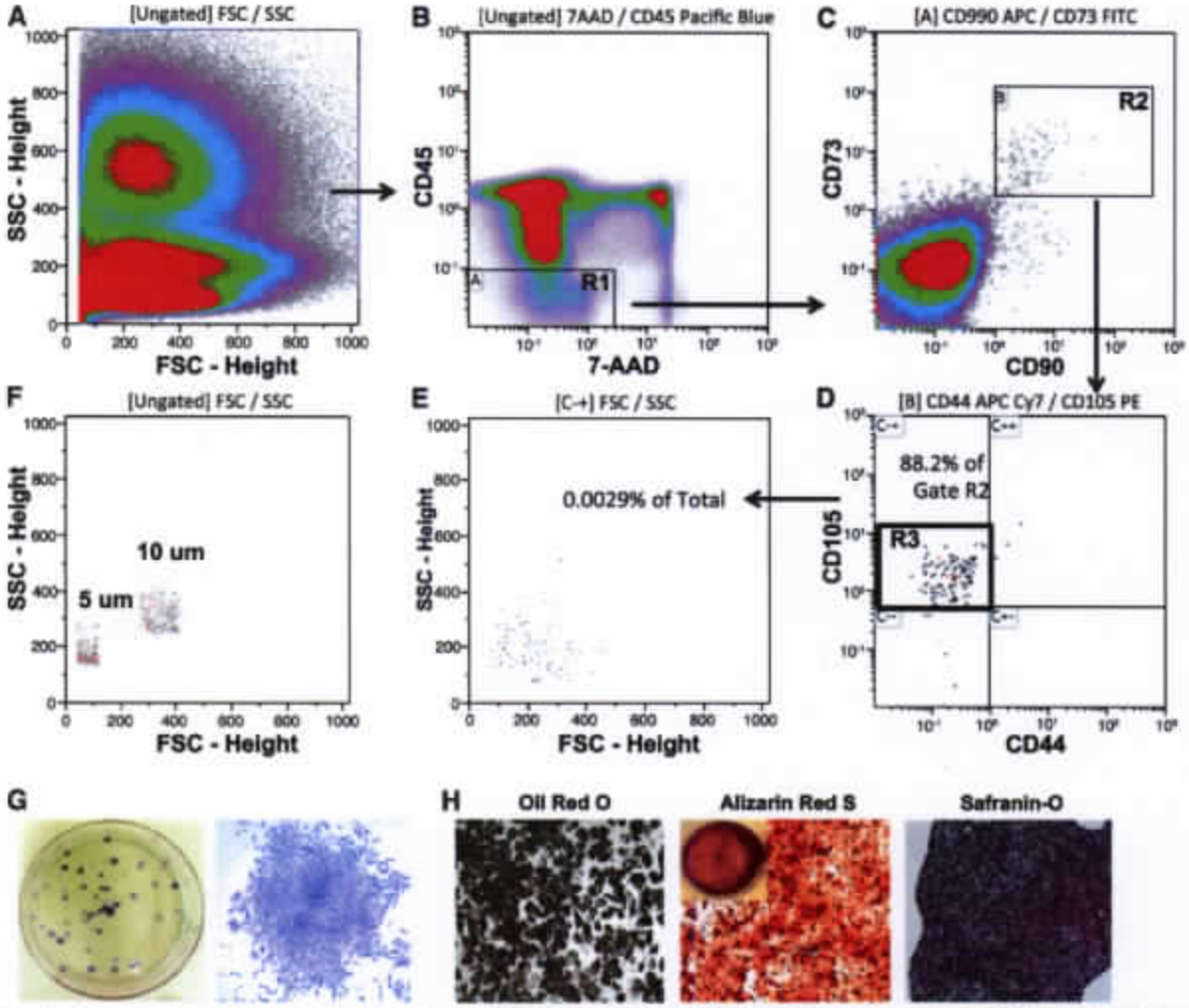

Figure 1. Prospective identification and isolation of small CD45$^-$CD73$^+$CD90$^+$CD105$^+$CD44$^-$ human bone marrow (BM) cells that behave as mesenchymal stem/stromal cells in culture using polychromatic flow cytometry/cell sorting. Using a five-antibody/viability marker panel, we identified a subset of small cells within fresh human BM that were negative for CD44$^-$. **(A, B):** Mononuclear cells were initially displayed on an SSC/FSC color density plot of BM cells **(A)**, which was subgated onto an antigen plot **(B)** for identification of CD45$^-$7-AAD$^-$ (live) cells (gate R1). **(C, D):** CD45$^-$7-AAD$^-$ cells were further subgated to display of a cluster of CD73$^+$CD90$^+$ cells (gate R2) **(C)**, which were then displayed as a quadrant gate **(D)** to identify the CD105$^+$CD44$^-$ subset of cells. The sort window of CD105$^+$CD44$^-$ cells is indicated as R3. **(E, F):** Back-gating of the original CD45$^-$CD73$^+$CD90$^+$CD105$^+$CD44$^-$ population revealed their location near the lymphocyte population within the SSC-height/FSC-height color density plot **(E)**, and standard-sized flow cytometric beads confirmed their small size (right) **(F)**. **(G):** Representative image of typical colony forming unit-fibroblast from CD45$^-$CD73$^+$CD90$^+$CD105$^+$CD44$^-$ sorted cells and higher power image of a single colony (×4, right). **(H):** Fluorescence-activated cell sorting-sorted CD44$^-$ cells were expanded in culture and demonstrated trilineage differentiation potential in vitro toward adipocytes detected using Oil Red O stain for lipids (×10, left), osteoblasts detected using alizarin red S stain (middle), and chondroblasts detected using safranin-O stain (right). Similar results were seen in four other BM samples from different donors. Abbreviations: 7-AAD, 7-aminoactinomycin D; FSC, forward scatter; SSC, side scatter.

sets when there were more than two groups for multiple comparisons. $p < .05$ was used as the significance level.

Results

Human Bone Marrow Contains a Population of Small CD45$^-$CD73$^+$CD90$^+$CD105$^+$ Cells That Lack CD44 but Exhibit Mesenchymal Stem/Progenitor Cell-Like Properties

The phenotype of human BM MSPCs in vivo is not known; therefore, a panel of antibodies representing the most common markers for plastic-adherent BM-MSCs was used for their prospective identification. This six-color panel, which includes antibodies to CD45, CD73, CD90, CD105, and CD44 and the cell viability marker 7-AAD, was used for fluorescence-activated cell sorting (FACS) to analyze CD34/CD133-depleted BM for populations that contain MSC activity. First, CD45$^-$7-AAD$^-$ (live, gate R1) cells were identified and subgated onto an antigen plot (Fig. 1A, 1B), where a rare population of CD73$^+$CD90$^+$ cells was identified as candidate MSCs (Fig. 1C, gate R2). Further subgating of the live (7-AAD$^-$) CD45$^-$CD73$^+$CD90$^+$ cells indicated that a large majority of these cells were CD105$^+$ but CD44$^-$ (Fig. 1D, gate R3). Remarkably, back-gating of the CD45$^-$CD73$^+$CD90$^+$CD105$^+$CD44$^-$ cells onto the SSC/FSC density plot revealed the location of these rare cells in a region where small cells are found (Fig. 1E). Microbeads

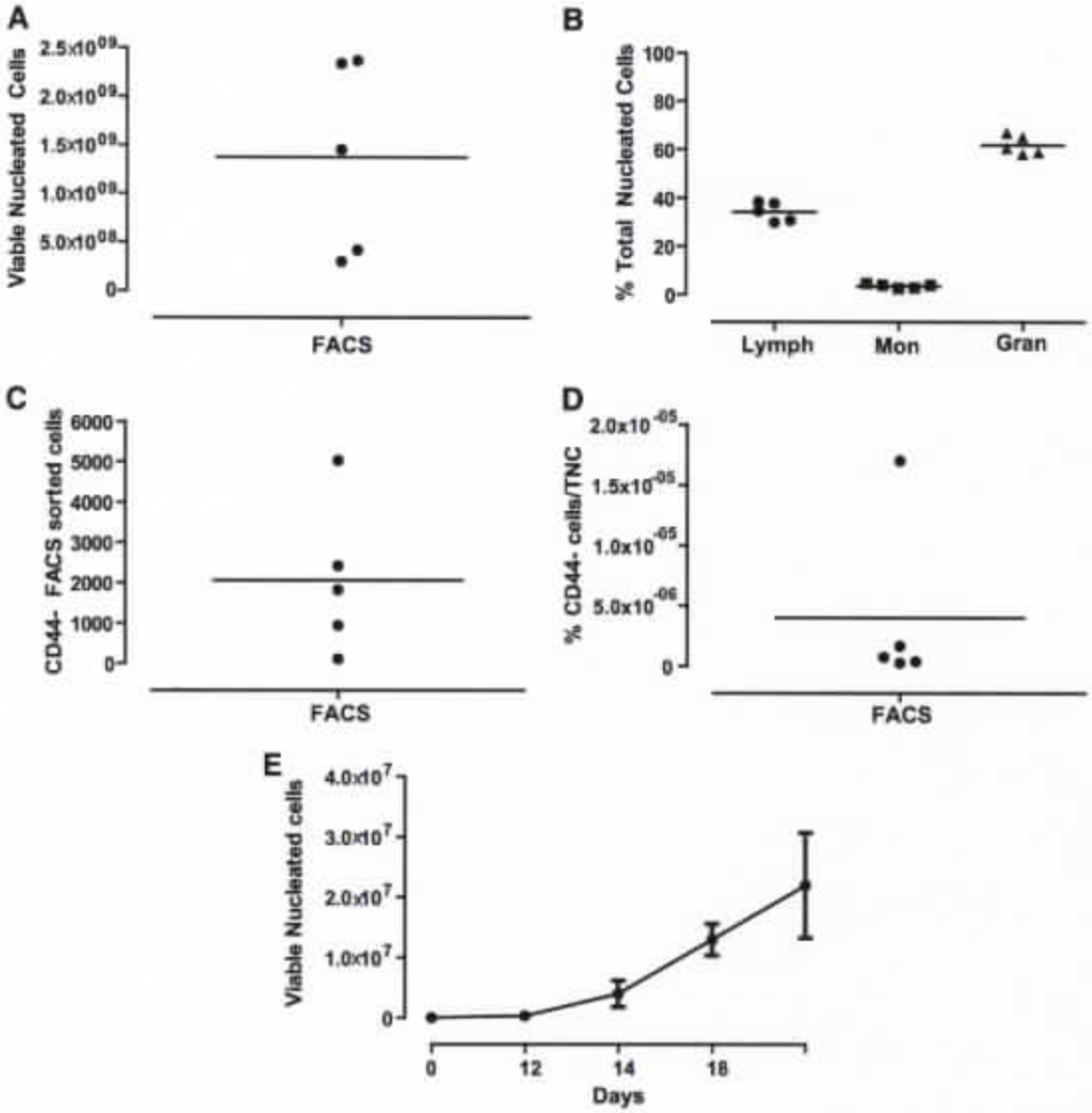

Figure 2. Characteristics of FACS CD44$^-$ fraction isolated from lysed bone marrow. **(A):** Viable nucleated cells obtained from lysed bone marrow from healthy donors. **(B):** Differential cell count compared with TNCs. **(C):** Number of sorted CD45$^-$CD73$^+$CD90$^+$CD105$^+$CD44$^-$ cells obtained from CD34/CD133-depleted bone marrow. **(D):** Percentage of CD45$^-$CD73$^+$CD90$^+$CD105$^+$CD44$^-$ cells normalized to TNCs. **(E):** Growth potential of CD45$^-$CD73$^+$CD90$^+$CD105$^+$CD44$^-$ cells over 21 days. Data are presented as mean ± SEM, $n = 5$. Differential cell counts were performed using an automated hematology analyzer (Beckman Coulter). Abbreviations: FACS, fluorescence-activated cell sorting; TNC, total nucleated cells.

of standard size demonstrate that the CD44$^-$ cells were between 5 and 12 μm (Fig. 1F). Proper placement of our gates was verified using "fluorescence minus one" controls (supplemental online Fig. 1). Next, the sorted CD45$^-$CD73$^+$CD105$^+$CD44$^-$ cells were plated onto plastic in chemically defined, serum-free medium (MSCGM-CD). Surprisingly, MSC activity, in the form of characteristic CFU-F, was found in the fraction lacking expression of CD44, widely considered an important MSC marker. The CD44$^-$ cells rapidly proliferated and formed characteristic CFU-F by day 12 (Fig. 1G). Following expansion, these cells were able to differentiate into osteoblasts, chondrocytes, and adipocytes under defined conditions in vitro (Fig. 1H), indicating that they function as MSPCs. Differential cell counts from the BM, final yield of the FACS-sorted CD44$^-$ fraction, and their growth potential are depicted in Figure 2A–2E.

Elutriation Enriches for CD44$^-$ MSPCs and Confirms Their Small Size

The unexpectedly small size of the FACS-sorted CD44$^-$ MSPCs led to studies to determine whether elutriation could be used to enrich these cells on the basis of their small size prior to FACS. CCE was used to separate lysed BM from healthy donor subjects into five distinct fractions on the basis of size. Platelets were removed almost entirely in the first elutriated fraction (35 ml/minute; fraction 35), which contained very few nucleated cells and was discarded. The cell yield and composition from all the subsequent collected fractions is shown in Figure 3A–3D. CCE was able to separate the lymphocyte population (fractions 70 and 90) from the granulocytes, which were collected primarily in the largest cell fractions (fractions 110 and >110), and to a lesser

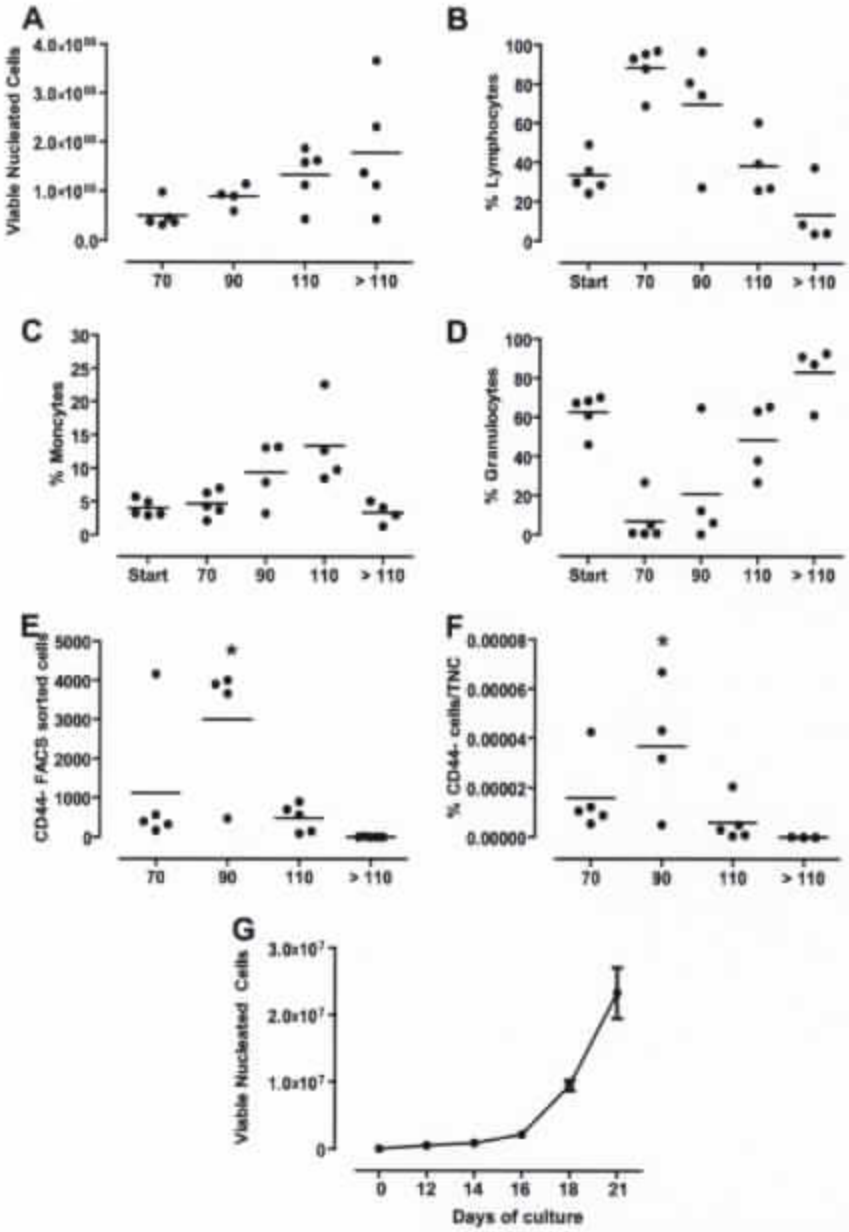

Figure 3. Characteristics of elutriated fractions from lysed bone marrow (BM). **(A–D):** Distribution of viable nucleated cells **(A)** and percentage of lymphocytes **(B)**, monocytes **(C)**, and granulocytes **(D)** recovered from the various fractions of lysed BM. **(E):** Quantification of FACS-sorted $CD44^-$ cells from the four fractions. Peak recovery was found in fraction 90. **(F):** The percentage of rare $CD45^-CD73^+CD90^+CD105^+CD44^-$ cells from the various fractions when normalized to TNCs demonstrated that fraction 90 contained the bulk of cells. $CD45^-CD73^+CD90^+CD105^+CD44^-$ cells from fraction 90 were sorted, and the cumulative growth curve **(G)** was calculated over 21 days after initial plating, calculated as day 0. Data are presented as mean ± SEM, $n = 5$. *, $p < .05$ versus fractions 100–110 and >110, using one-way analysis of variance followed by the Newman-Keuls multiple comparison test. Differential cell counts were performed using an automated hematology analyzer (Beckman Coulter). Abbreviations: FACS, fluorescence-activated cell sorting; TNC, total nucleated cells.

extent from monocytes. The majority of nucleated cells elutriated in the later fractions, with 45% of cells found in fraction >110 alone (Fig. 3A). The cell separation in each fraction based on size can also be seen by the change in the SSC/FSC pseudo-color density plots (Fig. 4A–4D). $CD45^-CD73^+CD90^+CD105^+CD44^-$ MSPCs were found in fraction 70 and peaked in fraction 90, confirming their small size (Figs. 3E, 4A–4D). The $CD44^-$ MSPC population was extremely rare, with approximately 1 in 25,000 events in fraction 90 being live $CD45^-CD73^+CD90^+CD105^+CD44^-$ cells (Fig. 3F). Despite their rarity, sorted cells from fraction 90 underwent a 10,000-fold expansion in culture 21 days after the initial sort (Fig. 3G).

$CD44^-$ MSPCs Expanded in Culture Acquire CD44 and Express Other Phenotypic Markers Characteristic of MSCs

To determine whether FACS-sorted $CD44^-$ MSPCs expanded in culture were phenotypically similar to conventional MSCs, elutriated/

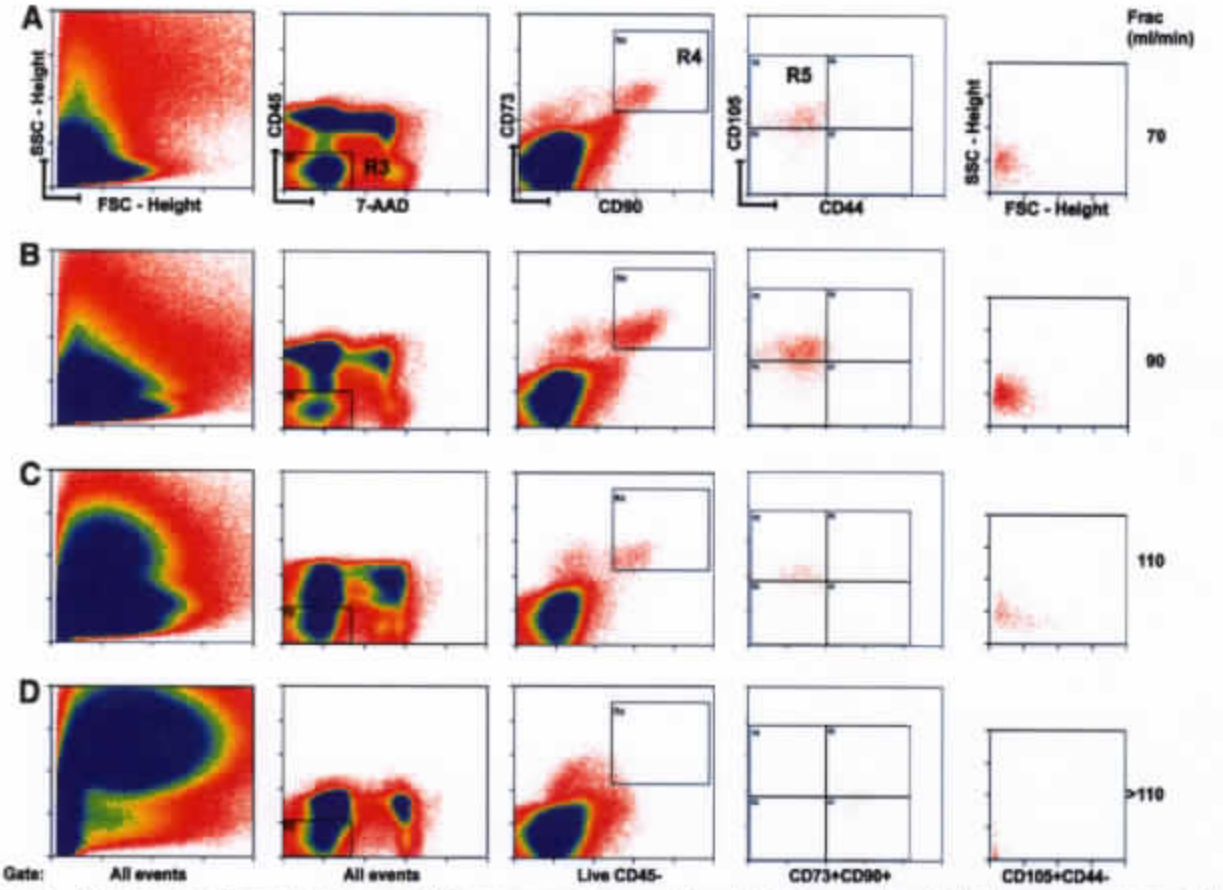

Figure 4. Fractionation of human bone marrow (BM) using counterflow centrifugal elutriation combined with fluorescence-activated cell sorting using the five-antibody/viability marker panel shows that $CD45^-CD73^+CD90^+CD105^+CD44^-$ MSPCs elute as small cells (70 and 90 ml/minute). **(A–D):** Representative display of SSC/FSC color density plots of the elutriated fractions 50/70 **(A)**, 90 **(B)**, 100–110 **(C)**, and >110 **(D)**. Display of CD45/7-AAD density plot was used to identify $CD45^-7\text{-}AAD^-$ (live) cells (gate R3), which was subgated onto a CD73/CD90 antigen plot and identified a cluster of live $CD45^-CD73^+CD90^+$ cells (gate R4), which was further subgated onto a CD105/CD44 antigen plot. Shown is the display of $CD105^+CD44^-$ on live $CD45^-CD73^+CD90^+$ gated cells. The sort window shows a cluster of $CD105^+CD44^-$ cells (R5). The sorted live $CD45^-CD73^+CD90^+CD105^+CD44^-$ cells (gate R5) are distributed close to the location of lymphocytes when back-gated onto an SSC-height/FSC-height dot plot (far right). Representative images from one experiment are shown. Similar results were seen in four other BM samples from different donors. Abbreviations: 7-AAD, 7-aminoactinomycin D; Frac, fraction; FSC, forward scatter; SSC, side scatter.

FACS-sorted $CD44^-$ cells from fraction 90 that had been cultured for three passages were compared with donor-matched MSCs isolated from BM by the conventional method of Ficoll purification followed by plastic adherence (Fig. 5). Single-color FACS analysis showed that the small, $CD45^-CD73^+CD90^+CD105^+CD44^-$ MSPCs acquired a higher CD44 expression following culture on plastic than conventionally purified MSCs. In addition, the cultured FACS-sorted cells expressed other typical markers reported for MSCs isolated by conventional methods, such as CD10, CD49d, CD49e, CD61, CD71, and CD146 (Fig. 5). Also similar to MSCs, the cultured cells from fraction 90 were negative for CD14, CD15, CD19, CD34, CD133, and HLA-DR. Both expanded MSPCs and conventional, cultured MSCs were negative for CD271 and STRO-1, two proteins that have been proposed as markers for the prospective isolation of MSCs from BM [26, 38, 39]. There were some differences between cells prepared by the two methods, notably in CD10, MSCA-1, CXCR4, CD56, CD54, and SSEA4, with perhaps MSCA-1 being the most prominent; however, the functional consequences of these differences are not clear (Fig. 5).

G-CSF Diminishes CD44 Expression in FACS-Sorted MSPCs but Not Conventional MSCs

There has been speculation about the concept that MSCs can mobilize from the BM and circulate in peripheral blood, yet there is little evidence in support of this controversial view [40]. To address this question, mobilized peripheral blood products obtained from healthy donors following a 3-day course of G-CSF were evaluated for the presence of rare $CD44^-$ cells using our method of either FACS or elutriation/FACS. However, only very rare $CD45^-CD73^+CD90^+CD105^+CD44^-$ cells were detected in a G-CSF-mobilized peripheral blood collected as an apheresis product (Fig. 6A). These cells were not expandable, either as a typical CFU-F or growth in a nonclonal fashion (data not shown).

The effects of G-CSF on the MSPC population were investigated further. In vitro culture of elutriated/FACS-sorted BM-derived $CD44^-$ cells resulted in acquisition of CD44 expression, which is sensitive to G-CSF (Fig. 6B, 6C). Treatment of culture-expanded MSPCs, derived from the $CD44^-$ fraction via elutriation/FACS, with recombinant human (rh) G-CSF (10 ng/ml) for 3

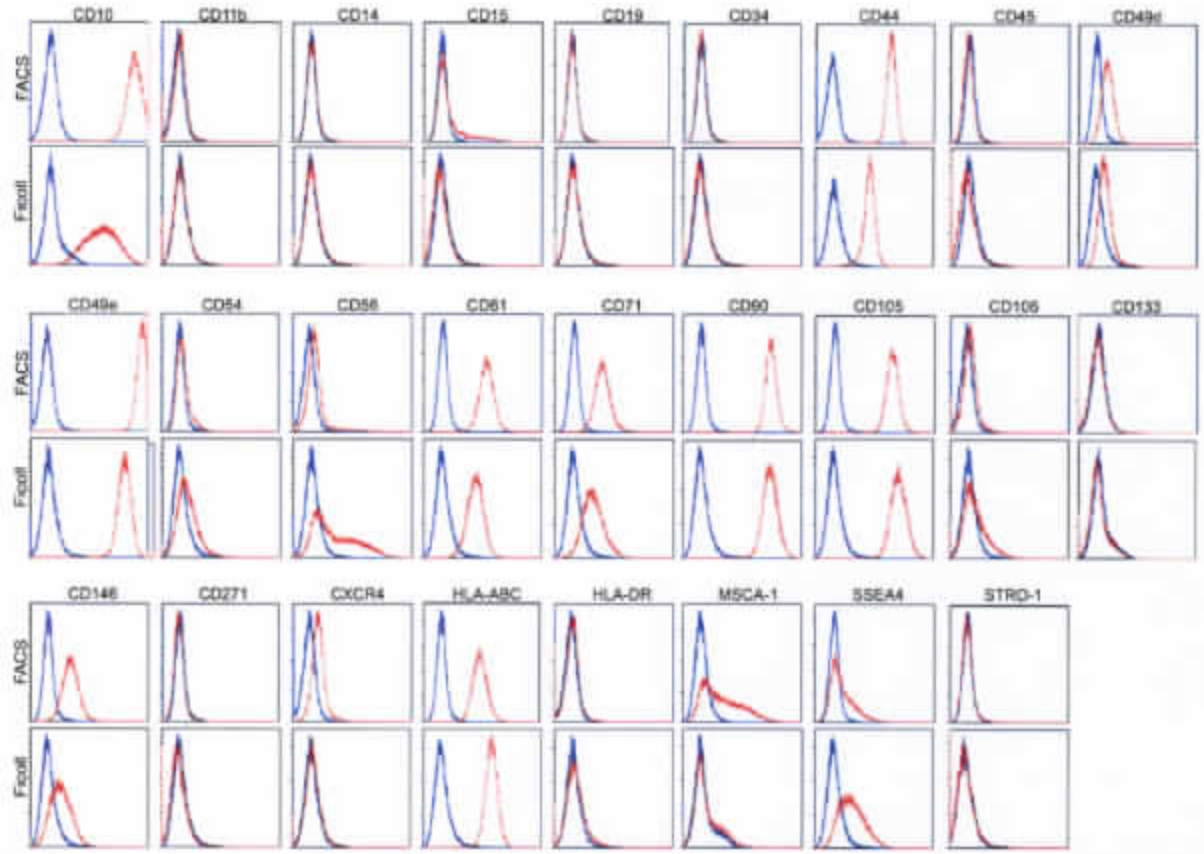

Figure 5. Immunophenotypic analysis of elutriated CD44$^-$ MSPCs. Single-color flow cytometric analysis of selected cell surface proteins on passage 3 culture-expanded CD45$^-$CD73$^+$CD90$^+$CD105$^+$CD44$^-$ cells (top panels in each row, FACS) compared with passage 3 donor-matched mesenchymal stem/stromal cells isolated using conventional methods (bottom panels in each row, Ficoll). Shown are representative images from one experiment. Similar results were seen in four other bone marrow samples from different donors. Blue line, isotype control; red line, primary antibody. Abbreviation: FACS, fluorescence-activated cell sorting.

consecutive days resulted in diminished expression of CD44, which was demonstrated by the appearance of a CD44^{lo} population (Fig. 6B) and quantified by a decrease in mean fluorescence intensity (MFI) compared with vehicle-treated cells ($3.2 \times 10^5 \pm 8.4 \times 10^4$ vs. $8.5 \times 10^5 \pm 1.1 \times 10^4$, respectively; $p < .037$) (Fig. 6C). In comparison, CD44 expression on culture-expanded donor-matched MSCs isolated using the conventional method was not altered following rhG-CSF treatment (MFI $2.4 \times 10^5 \pm 2.8 \times 10^4$ vs. $2.7 \times 10^5 \pm 1.4 \times 10^5$; not significant) (Fig. 6B, 6C).

CD44$^-$ MSPCs Exhibit a More Robust Expansion and Differentiation Capacity Compared With Conventionally Isolated MSCs

To further investigate the relative capacity of elutriated CD44$^-$ cells to expand and differentiate into tissues of mesenchymal lineage compared with conventionally isolated MSCs, differentiation assays were performed comparing elutriated/FACS-sorted CD44$^-$ cells from fraction 90 to donor-matched BM-MSCs prepared by Ficoll purification and plastic adherence. Both preparations were expanded in culture until passage 3. Representative colony appearance from elutriated/FACS-sorted cells on day 12 is shown in Figure 6A (left), as well as cell morphology after passage 1 (Fig. 7A, middle). Furthermore, elutriated/FACS-sorted CD44$^-$ cells demonstrated a greater expansion capacity over three passages compared with BM-MSCs isolated using the conventional method (Fig. 7A, right, $p < .041$). Following this, cells were used for the various differentiation assays in defined culture conditions in vitro.

After 21 days in osteogenic medium, sorted CD44$^-$ cells stained more densely with alizarin red S compared with conventional MSCs, indicating an enhanced mineralization in culture (Fig. 7B). In addition, pellets of CD44$^-$ cells expanded in chondrogenic induction medium for 21 days demonstrated more staining for safranin-O, a marker of cartilage, compared with donor-matched conventionally isolated MSCs (Fig. 7C). Finally, when plated in adipogenic medium, elutriated/FACS-sorted CD44$^-$ cells quickly acquired an adipogenic phenotype demonstrated by significant uptake of Oil Red O staining in lipid (Fig. 7D). Quantification of adipogenesis following isopropanol extraction of Oil Red O confirmed that CD44$^-$ MSPCs formed more lipid compared with conventionally isolated MSCs (Fig. 7D, far right) ($p < .034$).

Discussion

The data presented in this study demonstrate that a rare BM population of small, CD45$^-$CD73$^+$CD90$^+$CD105$^+$CD44$^-$ cells function as MSPCs. These MSPCs can readily be isolated from CD34/CD133-depleted BM by a combination of CCE and FACS. Once expanded in culture, these MSPCs acquire CD44 and exhibit a similar immunophenotype but a more robust expansion and

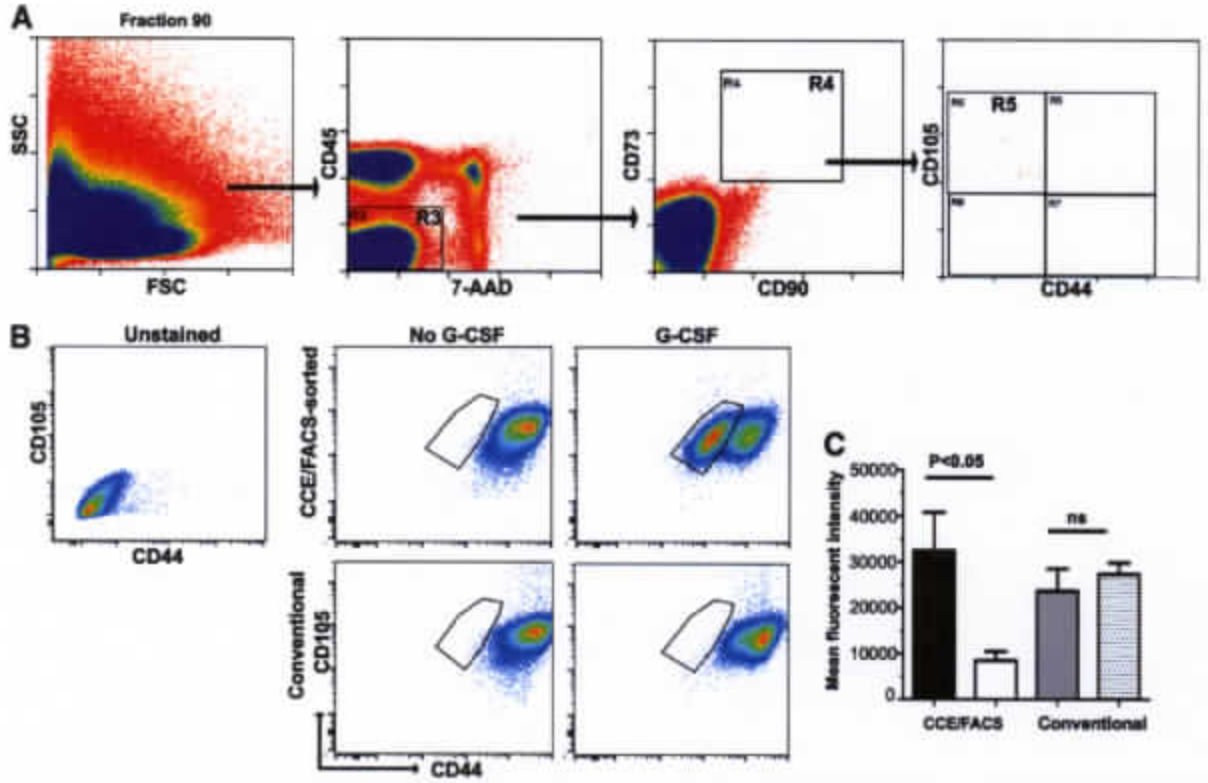

Figure 6. Detection of $CD45^-CD73^+CD90^+CD105^+CD44^-$ cells in G-CSF-mobilized peripheral blood, as previously defined in the bone marrow. **(A):** Representative display of flow cytometric density plots from fraction 90. Mononuclear cells were initially displayed on an SSC/FSC color density plot, which was subgated onto an antigen plot for identification of $CD45^-$ 7-AAD$^-$ (live) cells (gate R3). $CD45^-$ 7-AAD$^-$ cells were further subgated to identify $CD73^+CD90^+$ cells (gate R4), which were then displayed as a quadrant gate to identify $CD105^+CD44^-$ subset of cells (gate R5). The sort window of $CD105^+CD44^-$ cells is indicated as R5. **(B):** Representative flow cytometric density color plots showing the response of in vitro culture-expanded elutriated/FACS-sorted $CD44^-$ cells (top), which gain CD44 expression, versus conventionally isolated mesenchymal stem/stromal cells (MSCs) (bottom) following treatment with 10 ng/ml recombinant human (rh) G-CSF over 3 days. Treatment of in vitro culture-expanded CCE/FACS $CD44^-$ cells with rhG-CSF resulted in the appearance of a $CD44^{lo}$ subpopulation, whereas MSCs isolated using the conventional method of plastic adherence did not. **(C):** Change in mean fluorescence intensity is depicted as mean ± SEM, $n = 3$ independent experiments. *, $p < .05$ versus vehicle-treated cells using an unpaired t test. Abbreviations: 7-AAD, 7-aminoactinomycin D; CCE, counterflow centrifugal elutriation; FACS, fluorescence-activated cell sorting; FSC, forward scatter; G-CSF, granulocyte-colony stimulating factor; ns, not significant; SSC, side scatter.

differentiation potential compared with MSCs obtained by standard plastic adherence methods. Contrary to the widely held views that MSCs in vivo are large cells [38] and that CD44 represents a reliable and highly expressed marker on postcultivated BM-MSCs [39], our observations indicate that BM contains a primitive population of small MSPCs that simultaneously express CD73, CD90, and CD105 and lack CD44 and that the acquisition of CD44 expression is a postculture phenomenon.

There is a lack of consensus on the antigenic profile and morphology of bone marrow-derived MSPCs in vivo. Immunophenotypic analysis of conventionally isolated MSCs is generally performed following cultivation of cells that were initially selected on their ability to adhere to plastic. Although antibodies to several markers have been used for the prospective isolation of MSC subsets from BM, these studies have typically used a more limited number of antibodies in their marker panels [22, 23]. Introduction of a multicolor panel of antibodies (more than four colors) against more surface markers as presented here does appear to allow for better resolution of novel cell subsets and rare event analysis. Such multiparameter FACS procedures are widely used in the fields of hematopoietic [27] and endothelial stem and progenitor cell research [28].

Remarkably, the BM MSPCs identified in this study, as well as in a recent study by Qian et al. [40], lack expression of CD44, a multifunctional class I integral transmembrane glycoprotein that is widely expressed on a number of cells in the bone marrow with varying functions [41, 42]. In concordance with Qian et al., the $CD44^-$ cells in the present study acquired CD44 expression during culture, indicating that adherence and growth on plastic alters the in vivo antigenic profile of BM MSPCs. These observations underscore that markers found on culture-expanded BM-MSCs may not be present on their precursor cells in vivo. However, several differences between our observations are notable. First, Qian et al. [40] were able to identify a prominent $CD44^+$ fraction, which they were able to prospectively sort, and compare its CFU-F potential to that of the $CD44^-$ fraction. However, the $CD44^+$ fraction formed CFU-F only when plated at nonclonal densities of 2,000 cells per cm^2. Using a different antibody matrix and gating strategy, we did not detect a $CD44^+$ fraction, and therefore, we were not able to compare CFU-F potentials. Second, CD105 served as a key positive marker for the prospective isolation of $CD44^-$ MSPCs in our study. This is contrast to the report from Qian et al. [40], where CD105 expression was diminished or absent on primary $CD44^-$ cells. However, one study

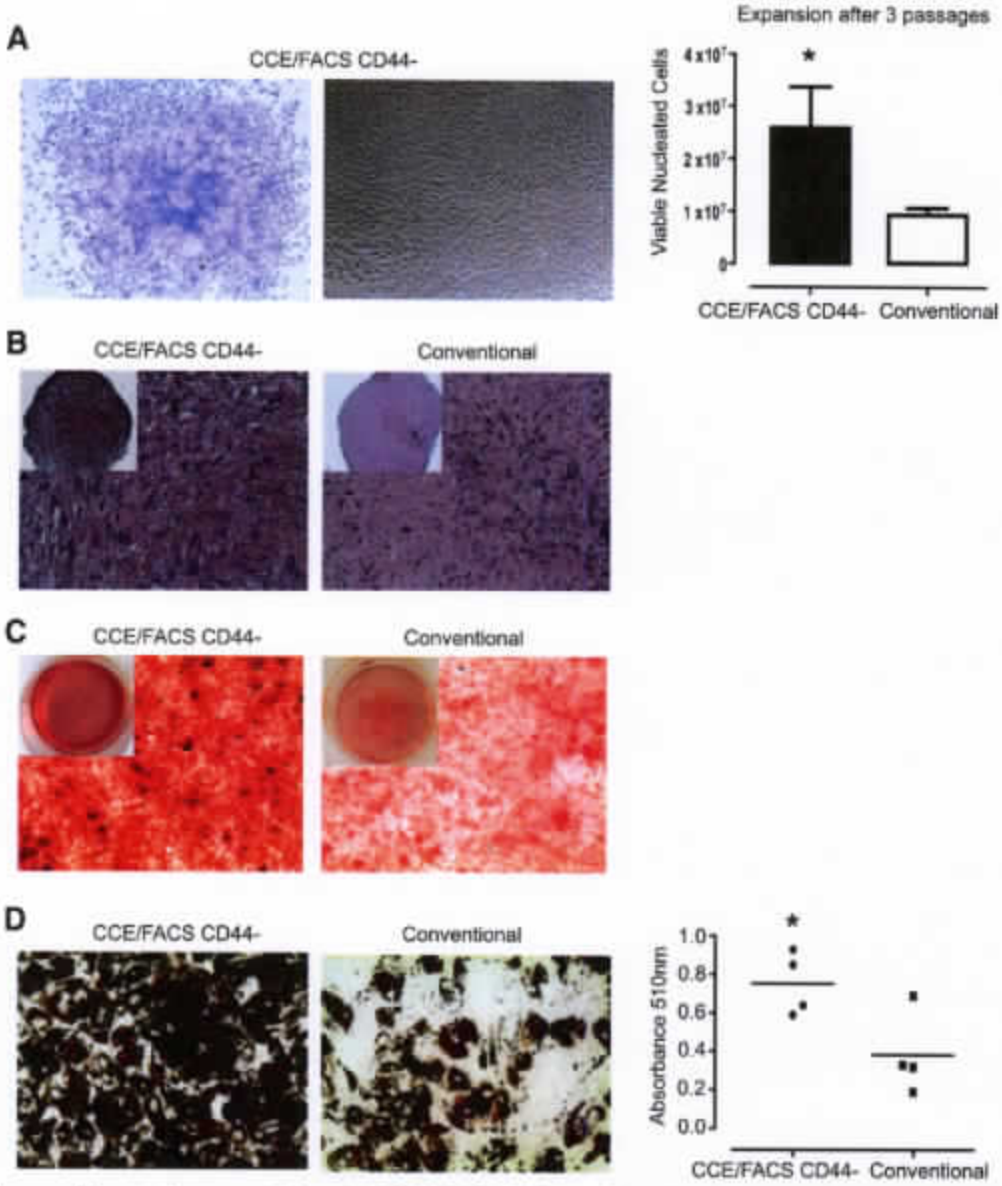

Figure 7. Trilineage differentiation potential of small CD45$^-$CD73$^+$CD90$^+$CD105$^+$CD44$^-$ cells obtained from fraction 90 following expansion. **(A):** In vitro growth of CCE/FACS CD44$^-$ cells obtained from fraction 90. Shown are a representative Giemsa-stained colony forming unit-fibroblast colony at day 12 (left) and the typical colony appearance by phase contrast (middle). After three passages, CCE/FACS-sorted cells demonstrated a greater expansion capacity compared with conventional mesenchymal stem/stromal cells (MSCs) (right). **(B–D):** After passage 3, cells were placed in differentiation conditions in vitro to induce osteogenesis, chondrogenesis, and adipogenesis. **(B):** To induce chondrogenesis, cell pellets were incubated with 10 ng/ml recombinant human transforming growth factor-β3. Chondrogenesis was detected following staining with safranin-O. A representative image of a CCE/FACS CD44$^-$ pellet (left) shows more intense staining compared with donor-matched conventional MSCs (right). **(C):** Osteogenesis was detected by staining cultures with 2% alizarin red S solution (pH 4.2). Shown is a representative image comparing osteogenesis cultures for CD44$^-$ cells (left) with cultures of donor-matched conventional MSCs (middle). The monolayer of CCE/FACS CD44$^-$ cells stained more densely with alizarin red S. **(D):** Adipogenesis was detected following staining of cultures with Oil Red O, which detects lipids. Representative images of CCE/FACS CD44$^-$ culture (left) compared with donor-matched conventional MSCs (middle) are shown (×20). Right panel shows spectrophotometric quantification of adipogenesis following isopropanol extraction of Oil Red O. Data are presented as mean ± SEM, $n = 4–5$. *, $p < .05$ versus conventional isolated MSCs, using an unpaired t test. Abbreviations: CCE, counterflow centrifugal elutriation; FACS, fluorescence-activated cell sorting.

reported that the administration of noncultured BM-derived cells immunoselected based entirely on CD105 expression resulted in robust bone formation through the endochondral pathway [43]. In addition to this difference in CD105 expression, the CD44$^-$ fraction identified by Qian et al. [40] coexpressed the low-affinity nerve growth factor receptor CD271 and STRO-1, markers that have previously been used to prospectively isolate cells with MSC-like potential [24–26, 44]. However, neither marker was shown to present on in vitro culture-expanded elutriated/FACS CD44$^-$ cells nor the donor-matched MSCs isolated using the conventional method. The stability of these markers in culture has been questioned and shown to be downregulated following expansion [45, 46]. However, there are conflicting reports describing this phenomenon [47]. At present, it is not

known whether the $CD44^-$ fraction discovered in our study using elutriation/FACS overlaps with the $CD44^-$ BM-MSPCs cells described by Qian et al. [40], and this will be the subject of future investigations.

Since there is a lack of data concerning the physical size of MSPCs within the BM, it was not known where these cells would fractionate using CCE. We anticipated that MSPCs may elutriate in the later fractions, which contain contaminating monocytes and granulocytes, as MSCs are suggested to be large cells in vivo [38]. However, the $CD44^-$ MSPCs were enriched in early fractions (Fig. 3) that also contain other stem and progenitor cell populations such as HSCs and very small embryonic-like stem cells, a population of developmentally early stem cells residing in adult tissues [48]. A previous study in mice similarly demonstrated that BM cells from the earliest elutriated fractions using CCE were endowed with a primitive potential and contribute to multiple tissues in recipient mice [36, 37]. Colter et al. also reported the presence of small, rapidly self-renewing cells isolated from human BM that demonstrated robust differentiation for both osteocytes or adipocytes [21]. In a follow-up study, MSCs were isolated on the basis of the FS^{lo}/SS^{lo} property, which enabled the enrichment of these small rapidly proliferating cells [49]. However, it is not known whether these cells, which appear to be early progenitors based on size, represent the same population as identified here, as the antigenic profile of these cells was not determined prior to plating. In further support of our finding, Rasini et al. recently demonstrated the existence of small, round/polygonal $CD73^+CD45^-$ cells in the BM stroma that are positive for a number of pluripotency markers [50]. These findings reinforce the need for a continued assessment of the human BM for putative MSC subpopulations and importantly, to link these cells with in vivo function.

Recent evidence indicates that MSCs play a supportive role in maintaining HSCs in a specialized niche within the BM [19]. This raises the question of whether MSCs, along with HSCs, may be mobilized by G-CSF from the BM to the peripheral circulation. The concept that MSCs mobilize and circulate remains controversial [51] with a lack of supportive evidence [40]. BM-MSCs respond to G-CSF by promoting the transmigration of $CD34^+$ cells in culture [52]. Using our method of FACS or elutriation/FACS, very rare $CD45^-CD73^+CD90^+CD105^+CD44^-$ cells could be detected in G-CSF mobilized peripheral blood products obtained from healthy donors; however, in our hands, these cells did not expand. In contrast, FACS or elutriation/FACS culture-expanded $CD44^-$ cells do respond to G-CSF, with loss of their acquired CD44 expression, an observation that was not seen with conventionally plastic purified MSCs (Fig. 6). The physiological significance and biological consequences of this difference are not known. Whether $CD44^-$ MSPCs might mobilize in response to other combinations of cytokines and growth factors remains to be determined [53].

Conclusion

In summary, we report here a distinct subset of small, highly proliferative MSPCs within human BM that lack CD44 but that exhibit mesenchymal-like multilineage differentiation capabilities. CCE represents a method that can enrich MSPCs from the BM; it also has the potential to obviate the need to FACS sort cells, since major contaminating populations of plastic-adherent cells such as monocytes are largely depleted by elutriation and could easily be completely removed by CD14 immunodepletion. In vivo studies are now needed to determine the fate and function of these MSPCs in normal tissue homeostasis and in various disease conditions, as well as to assess their therapeutic potential.

Acknowledgments

We thank Anthony Salerno for his enthusiastic support of this work. This study was funded by NeoStem, Inc.

Author Contributions

S.R.R.H.: conception and design, collection and/or assembly of data, data analysis and interpretation, manuscript writing; Y.J.: conception and design, collection and/or assembly of data, data analysis and interpretation; E.L. and G.Y.: collection and/or assembly of data; S.E.: data analysis and interpretation; D.W.O.: collection and/or assembly of data, data analysis and interpretation, manuscript writing; W.A.M.: conception and design, data analysis and interpretation, manuscript writing, final approval of manuscript.

Disclosure of Potential Conflicts of Interest

W.A.M. owns stock in NeoStem and was a paid consultant during this study, and G.Y. and D.W.O. have compensated employment from NeoStem.

References

1 Keating A. Mesenchymal stromal cells. Curr Opin Hematol 2006;13:419–425.

2 Bianco P, Robey PG, Simmons PJ. Mesenchymal stem cells: Revisiting history, concepts, and assays. Cell Stem Cell 2008;2:313–319.

3 Friedenstein AJ, Gorskaja JF, Kulagina NN. Fibroblast precursors in normal and irradiated mouse hematopoietic organs. Exp Hematol 1976;4:267–274.

4 Friedenstein AJ, Deriglasova UF, Kulagina NN et al. Precursors for fibroblasts in different populations of hematopoietic cells as detected by the in vitro colony assay method. Exp Hematol 1974;2:83–92.

5 Gronthos S, Arthur A, Bartold PM et al. A method to isolate and culture expand human dental pulp stem cells. Methods Mol Biol 2011; 698:107–121.

6 Jarvinen L, Badri L, Wettlaufer S et al. Lung resident mesenchymal stem cells isolated from human lung allografts inhibit T cell proliferation via a soluble mediator. J Immunol 2008; 181:4389–4396.

7 Lama VN, Smith L, Badri L et al. Evidence for tissue-resident mesenchymal stem cells in human adult lung from studies of transplanted allografts. J Clin Invest 2007;117:989–996.

8 Zannettino AC, Paton S, Arthur A et al. Multipotential human adipose-derived stromal stem cells exhibit a perivascular phenotype in vitro and in vivo. J Cell Physiol 2008;214: 413–421.

9 Igura K, Zhang X, Takahashi K et al. Isolation and characterization of mesenchymal progenitor cells from chorionic villi of human placenta. Cytotherapy 2004;6:543–553.

10 Kim HS, Shin TH, Yang SR et al. Implication of NOD1 and NOD2 for the differentiation of multipotent mesenchymal stem cells derived from human umbilical cord blood. PLoS One 2010;5:e15369.

11 da Silva Meirelles L, Caplan AI, Nardi NB. In search of the in vivo identity of mesenchymal stem cells. Stem Cells 2008;26:2287–2299.

12 Psaltis PJ, Carbone A, Nelson AJ et al. Reparative effects of allogeneic mesenchymal

precursor cells delivered transendocardially in experimental nonischemic cardiomyopathy. JACC Cardiovasc Interv 2010;3:974–983.

13 Lee JW, Gupta N, Serikov V et al. Potential application of mesenchymal stem cells in acute lung injury. Expert Opin Biol Ther 2009; 9:1259–1270.

14 Bartosh TJ, Ylostalo JH, Mohammadipoor A et al. Aggregation of human mesenchymal stromal cells (MSCs) into 3D spheroids enhances their antiinflammatory properties. Proc Natl Acad Sci USA 2010;107:13724–13729.

15 Uccelli A, Prockop DJ. Why should mesenchymal stem cells (MSCs) cure autoimmune diseases? Curr Opin Immunol 2010;22:768–774.

16 Uccelli A, Moretta L, Pistoia V. Mesenchymal stem cells in health and disease. Nat Rev Immunol 2008;8:726–736.

17 Le Blanc K, Ringden O. Immunomodulation by mesenchymal stem cells and clinical experience. J Intern Med 2007;262:509–525.

18 Castro-Malaspina H, Gay RE, Resnick G et al. Characterization of human bone marrow fibroblast colony-forming cells (CFU-F) and their progeny. Blood 1980;56:289–301.

19 Bianco P. Minireview: The stem cell next door: Skeletal and hematopoietic stem cell "niches" in bone. Endocrinology 2011;152: 2957–2962.

20 Pevsner-Fischer M, Levin S, Zipori D. The origins of mesenchymal stromal cell heterogeneity. Stem Cell Rev 2011;7:560–568.

21 Colter DC, Sekiya I, Prockop DJ. Identification of a subpopulation of rapidly self-renewing and multipotential adult stem cells in colonies of human marrow stromal cells. Proc Natl Acad Sci USA 2001;98:7841–7845.

22 Keating A. Mesenchymal stromal cells: New directions. Cell Stem Cell 2012;10:709–716.

23 Harichandan A, Buhring HJ. Prospective isolation of human MSC. Best Pract Res Clin Haematol 2011;24:25–36.

24 Tormin A, Li O, Brune JC et al. CD146 expression on primary nonhematopoietic bone marrow stem cells is correlated with in situ localization. Blood 2011;117:5067–5077.

25 Sacchetti B, Funari A, Michienzi S et al. Self-renewing osteoprogenitors in bone marrow sinusoids can organize a hematopoietic microenvironment. Cell 2007;131:324–336.

26 Churchman SM, Ponchel F, Boxall SA et al. Transcriptional profile of native CD271+ multipotential stromal cells: Evidence for multiple fates, with prominent osteogenic and Wnt pathway signaling activity. Arthritis Rheum 2012;64:2632–2643.

27 Notta F, Doulatov S, Laurenti E et al. Isolation of single human hematopoietic stem cells capable of long-term multilineage engraftment. Science 2011;333:218–221.

28 Mund JA, Estes ML, Yoder MC et al. Flow cytometric identification and functional characterization of immature and mature circulating endothelial cells. Arterioscler Thromb Vasc Biol 2012;32:1045–1053.

29 Banfalvi G. Cell cycle synchronization of animal cells and nuclei by centrifugal elutriation. Nat Protoc 2008;3:663–673.

30 Lindahl PE. On counter streaming centrifugation in the separation of cells and cell fragments. Biochim Biophys Acta 1956;21: 411–415.

31 Lindahl PE. Principle of a counterstreaming centrifuge for the separation of particles of different sizes. Nature 1948;161:648.

32 Wahl LM, Katona IM, Wilder RL et al. Isolation of human mononuclear cell subsets by counterflow centrifugal elutriation (CCE). I. Characterization of B-lymphocyte-, T-lymphocyte-, and monocyte-enriched fractions by flow cytometric analysis. Cell Immunol 1984; 85:373–383.

33 Powell DJ Jr., Brennan AL, Zheng Z et al. Efficient clinical-scale enrichment of lymphocytes for use in adoptive immunotherapy using a modified counterflow centrifugal elutriation program. Cytotherapy 2009;11:923–935.

34 Eifler RL, Lind J, Falkenhagen D et al. Enrichment of circulating tumor cells from a large blood volume using leukapheresis and elutriation: Proof of concept. Cytometry B Clin Cytom 2011;80:100–111.

35 Dlubek D, Dybko J, Wysoczanska B et al. Enrichment of normal progenitors in counterflow centrifugal elutriation (CCE) fractions of fresh chronic myeloid leukemia leukapheresis products. Eur J Haematol 2002;68:281–288.

36 Jones RJ, Collector MI, Barber JP et al. Characterization of mouse lymphohematopoietic stem cells lacking spleen colony-forming activity. Blood 1996;88:487–491.

37 Krause DS, Theise ND, Collector MI et al. Multi-organ, multi-lineage engraftment by a single bone marrow-derived stem cell. Cell 2001;105:369–377.

38 Jones E, McGonagle D. Human bone marrow mesenchymal stem cells in vivo. Rheumatology (Oxford) 2008;47:126–131.

39 Boxall SA, Jones E. Markers for characterization of bone marrow multipotential stromal cells. Stem Cells Int 2012;2012:975871.

40 Qian H, Le Blanc K, Sigvardsson M. Primary mesenchymal stem and progenitor cells from bone marrow lack expression of CD44 protein. J Biol Chem 2012;287:25795–25807.

41 Ponta H, Sherman L, Herrlich PA. CD44: From adhesion molecules to signalling regulators. Nat Rev Mol Cell Biol 2003;4:33–45.

42 Sackstein R, Merzaban JS, Cain DW et al. Ex vivo glycan engineering of CD44 programs human multipotent mesenchymal stromal cell trafficking to bone. Nat Med 2008;14:181–187.

43 Aslan H, Zilberman Y, Kandel L et al. Osteogenic differentiation of noncultured immunoisolated bone marrow-derived CD105+ cells. Stem Cells 2006;24:1728–1737.

44 Simmons PJ, Torok-Storb B. Identification of stromal cell precursors in human bone marrow by a novel monoclonal antibody, STRO-1 Blood 1991;78:55–62.

45 Jones EA, Kinsey SE, English A et al. Isolation and characterization of bone marrow multipotential mesenchymal progenitor cells. Arthritis Rheum 2002;46:3349–3360.

46 Jones E, English A, Churchman SM et al. Large-scale extraction and characterization of CD271+ multipotential stromal cells from trabecular bone in health and osteoarthritis: Implications for bone regeneration strategies based on uncultured or minimally cultured multipotential stromal cells. Arthritis Rheum 2010;62:1944–1954.

47 Battula VL, Treml S, Bareiss PM et al. Isolation of functionally distinct mesenchymal stem cell subsets using antibodies against CD56, CD271, and mesenchymal stem cell antigen-1. Haematologica 2009;94:173–184.

48 Ratajczak MZ, Zuba-Surma EK, Wysoczynski M et al. Very small embryonic-like stem cells: Characterization, developmental origin, and biological significance. Exp Hematol 2008; 36:742–751.

49 Smith JR, Pochampally R, Perry A et al. Isolation of a highly clonogenic and multipotential subfraction of adult stem cells from bone marrow stroma. Stem Cells 2004;22:823–831.

50 Rasini V, Dominici M, Kluba T et al. Mesenchymal stromal/stem cells markers in the human bone marrow. Cytotherapy 2013;15: 292–306.

51 Prockop DJ. Marrow stromal cells as stem cells for nonhematopoietic tissues. Science 1997;276:71–74.

52 Ponte AL, Ribeiro-Fleury T, Chabot V et al. Granulocyte-colony-stimulating factor stimulation of bone marrow mesenchymal stromal cells promotes CD34+ cell migration via a matrix metalloproteinase-2-dependent mechanism. Stem Cells Dev 2012;21:3162–3172.

53 Hoggatt J, Pelus LM. Many mechanisms mediating mobilization: An alliterative review. Curr Opin Hematol 2011;18:231–238.

See www.StemCellsTM.com for supporting information available online.

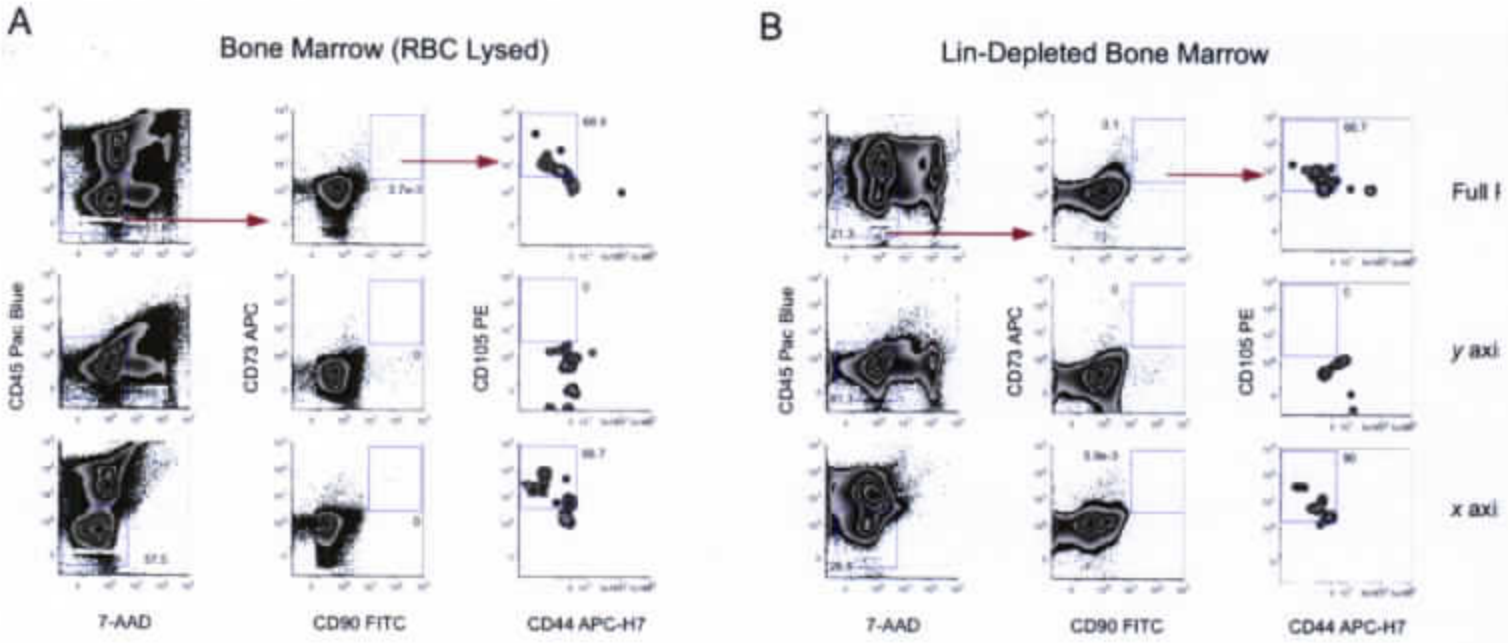
A
Bone Marrow (RBC Lysed)
B
Lin-Depleted Bone Marrow
CD45 Pac Blue
CD73 APC
CD105 PE
7-AAD
CD90 FITC
CD44 APC-H7
Full I
y axi
x axi

Table S1. List of antibodies used

Antibody	Color Conjugate	Clone	Isotype	Vendor	Cat#
HLA-ABC	FITC	G46-2.6	Mouse IgG2a,κ	BD Pharmingen	555552
HLA-DR	APC	G46-2	Mouse IgG2a,κ	BD Pharmingen	560896
CD10	APC	HI10a	Mouse IgG1,κ	BioLegend	312210
CD11b	APC	ICRF44	Mouse IgG1,κ	BD Pharmingen	550019
CD14	FITC	M5E2	Mouse IgG2a,κ	BD Pharmingen	555397
CD15	FITC	HI98	Mouse IgG1,κ	BD Pharmingen	555401
CD19	FITC	HIB19	Mouse IgG1,κ	BD Pharmingen	555412
CD34	APC	581	Mouse IgG1,κ	BD Pharmingen	560941
CD44	APC-H7	G44-26	Mouse IgG2a,κ	BD Pharmingen	560532
CD45	PB	J.33		Beckman Coulter	A74765
CD49d	FITC	9F10	Mouse IgG1,κ	BD Pharmingen	560840
CD49e	APC	NKI-SAM-1	Mouse IgG2b,κ	BioLegend	328012
CD54	FITC	84H10	Mouse IgG1,κ	Beckman Coulter	IM076U
CD56	PB	HCD56	Mouse IgG1,κ	BioLegend	318326
CD61	FITC	V1-PL2	Mouse IgG1,κ	BD Pharmingen	555753
CD71	FITC	M-A712	Mouse IgG2a,κ	BD Pharmingen	561938
CD73	APC	AD2	Mouse IgG1,κ	BD Pharmingen	560847
CD73	PE-Cy7	AD2	Mouse IgG1,κ	BD Pharmingen	561258
CD90	FITC	5E10	Mouse IgG1,κ	BD Pharmingen	555595
CD90	PE	5E10	Mouse IgG1,κ	BD Pharmingen	555596
CD105	PE	266	Mouse IgG1,κ	BD Pharmingen	560839
CD105	PE	SN6	Mouse IgG1,κ	Invitrogen	MHCD10504
CD106	APC	51-10CP	Mouse IgG1,κ	BD Pharmingen	551147
CD133	APC	AC133	Mouse	Miltenyi	130-090-826

			IgG1,κ		
CD146	PE	P1H12	Mouse IgG1,κ	BD Pharmingen	530315
CD271	PE	ME20.4	Mouse IgG1,κ	Miltenyi	130-093-819
CD271	APC	ME20.4	Mouse IgG1,κ	Miltenyi	130-092-283
CXCR4	APC	12G5	Mouse IgG2a,κ	BD Pharmingen	555976
MSCA1	FITC	W8B2	Mouse IgG1,κ	Miltenyi	130-093-587
MSCA1	APC	W8B2	Mouse IgG1,κ	Miltenyi	130-093-589
SSEA4	AlexaFluor 647	MC813-70	Mouse IgG3,κ	BD Pharmingen	560219
STRO-1	FITC	STRO1	Mouse IgGM	BioLegend	340105

2

Supplemental Information

Materials and Methods

BM obtained from healthy donors (Lonza, MD) underwent RBCs lysis (1X Pharm Lyse buffer, BD Biosciences) and afterwards were washed and counted for viability and resuspended in DPBS or Stain Buffer-FBS (BD Biosciences) for flow cytometric staining. In a separate experiment, lineage-committed hematopoietic cells were depleted using a lineage depletion kit (Human Progenitor Cell Enrichment Kit, StemCell Technologies, Canada). Unstained cells and isotype stained control samples were used to set PMT voltage for baseline fluorescence and to set quadrant statistics for analyzing positive fluorescence above baseline. Compensation was performed using known positive single color stained samples together with an unstained control. To avoid gating errors when staining with multiple colors, fluorescent minus one gating controls were used. Data acquisition and analysis on the MoFlo cell sorter was performed using Summit Software (Beckman Coulter). Data acquisition on the Gallios flow cytometer was performed uncompensated using Gallios system software, with compensation and analysis performed using FloJo (Tree Star, Ashland, OR).. The following primary conjugated monoclonal antibodies were used: CD45-pacific blue (PB; Beckman Coulter), CD73-allophycocyanin (APC; BD Biosciences), CD90-fluorescein isothiocyanate (FITC; BD Biosciences and BioLegend), CD105-phycoerythrin (PE; BD Biosciences) and CD44-allophycocyanin H7 (APC-H7; BD Biosciences). Following staining, cells were washed with DPBS or Stain Buffer-FBS and re-suspended in the same buffer. The viability dye 7-Aminoactinomycin D (7-AAD; Beckman Coulter) was added prior to analysis.

Figure S1. Bi-exponential scaling and fluorescent minus one (FMO) gating controls help to identify rare $CD45^-CD73^+CD90^+CD105^+CD44^-$ human BM cells. Representative polychromatic flow cytometric analysis of human BM preparation stained with the 5 antibody/viability marker panel and appropriate FMO controls. (A) Lysed BM was gated onto a bi-variant antigen plot for identification of $CD45^-$7-AAD^- (live) cells (top row, left panel, blue rectangle). $CD45^-$7-AAD^- cells were further subgated onto another bi-variant antigen plot to display a cluster of $CD73^+CD90^+$ cells (top row, middle panel, blue rectangle). Live $CD45^-CD73^+CD90^+$ cells were subgated onto a final bi-variant antigen plot for the identification of $CD105^+CD44^-$ cells (top right panel, blue rectangle). Accurate placement of gates based on FMO controls is depicted in the middle and lower rows. Plots in the middle row (from left to right) correspond to parallel samples stained without CD45, CD73 and CD105 antibodies, respectively. Plots in the lower row correspond to parallel samples stained without 7-AAD, CD90 and CD44. (B) Detection of $CD45^-CD73^+CD90^+CD105^+CD44^-$ cells was not different when bone marrow was depleted of lineage-committed hematopoietic cells (top panels). Furthermore, FMO controls also demonstrate the proper placement of gates to identify rare cells when using multicolor staining (middle and lower panels).